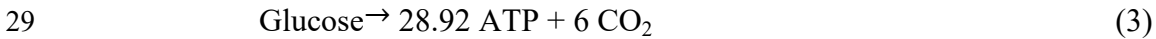
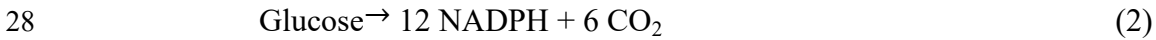
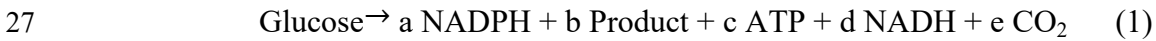


19 Supplementary Note

20 Yield calculation

21 The yield calculation is based on the methods described previously by Deepak Dugar *et al.* ¹.
22 Theoretical maximum yield (Y^E) is the maximum amount of a product produced from the
23 carbon source, which is merely calculated from the ratios of degree of reduction of substrate
24 to that of product. The theoretical pathway yield (Y^p) is the maximum amount of a product
25 produced by a specified pathway from its stoichiometry, which can be resolved from the
26 following equations:



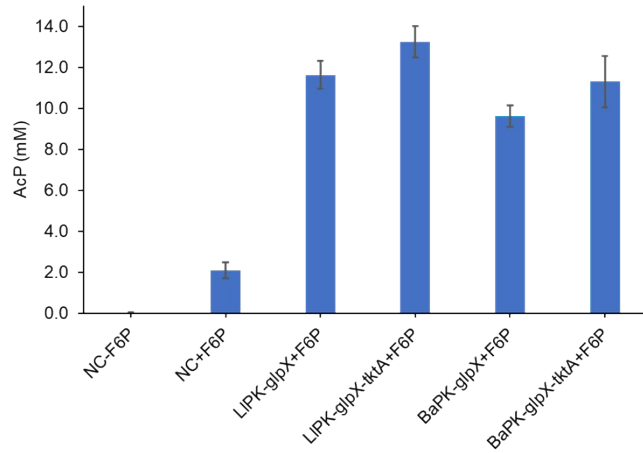
30

31 The theoretical pathway yield (Y^p) can be calculated with

32
$$Y^p = Y * \frac{1}{1 - a/12 - c/28.92}$$
 (4)

33 Y is product yield based on equation (1) ($Y=b$). When $a>0$, which means NADPH is excessive,
34 a is assigned 0 in the equation (4); when $c>0$, which means ATP is abundant, c is assigned 0
35 in the equation (4). To calculate Y^p without cofactor imbalance, in which case NADH and
36 NADPH are interconvertible, a is assigned $(a+c)$ if $(a+c)<0$, otherwise a is assigned 0 in the
37 equation (4).

38



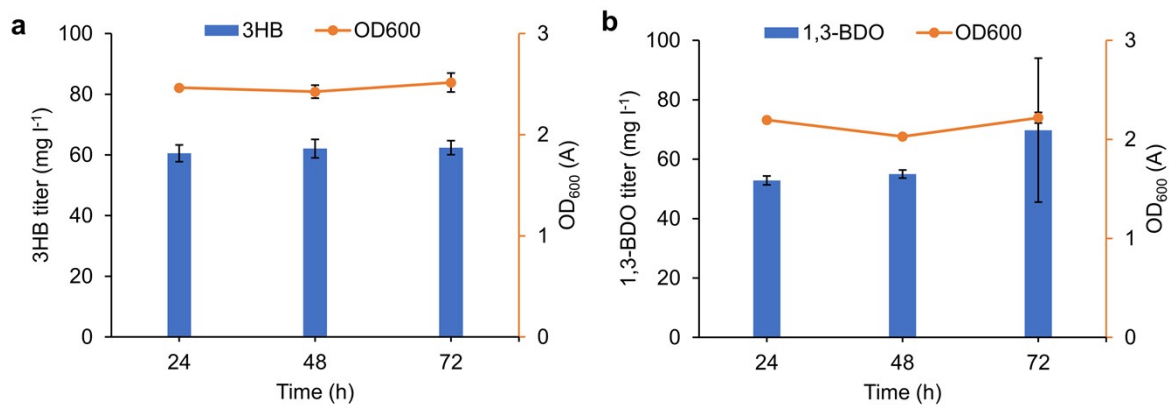
39

40 **Fig. S1.** Enzyme assay of F6P-to-AcP conversion using crude enzyme extracts of wildtype *E.*
 41 *coli* BW25113 (F') harboring empty plasmid pZE12-luc (NC, negative control), expressing
 42 BaPK and *glpX* (BaPK-*glpX*), expressing BaPK, *glpX* and *tktA* (BaPK-*glpX*-*tktA*), expressing
 43 LIPK and *glpX* (LIPK-*glpX*), expressing LIPK, *glpX* and *tktA* (LIPK-*glpX*-*tktA*). 10 mM F6P
 44 was added as the substrate. Data indicated the mean \pm standard deviation ($n = 3$ independent
 45 biological replicates).

46

47

48

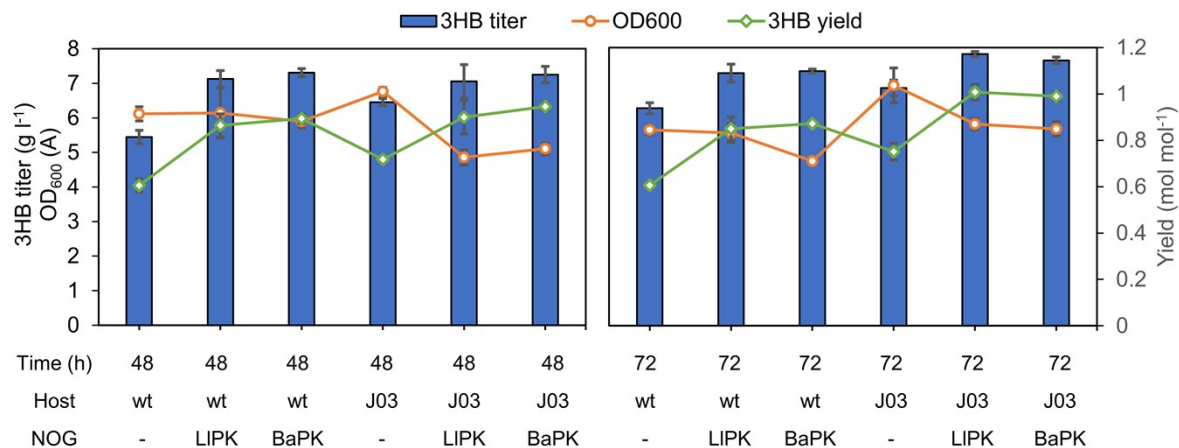


49

50 **Fig. S2.** Shake flask experiments with M9 medium with 5 g l⁻¹ yeast extract without
 51 glucose in 72 h. (a) 3HB production with *E. coli* BW25113 (F') harboring p3HB. (b) 1,3-BDO
 52 production with *E. coli* BW25113 (F') harboring p3HB and pZE-MaCAR. Data indicated the
 53 mean \pm standard deviation ($n = 3$ independent biological replicates).

54

55

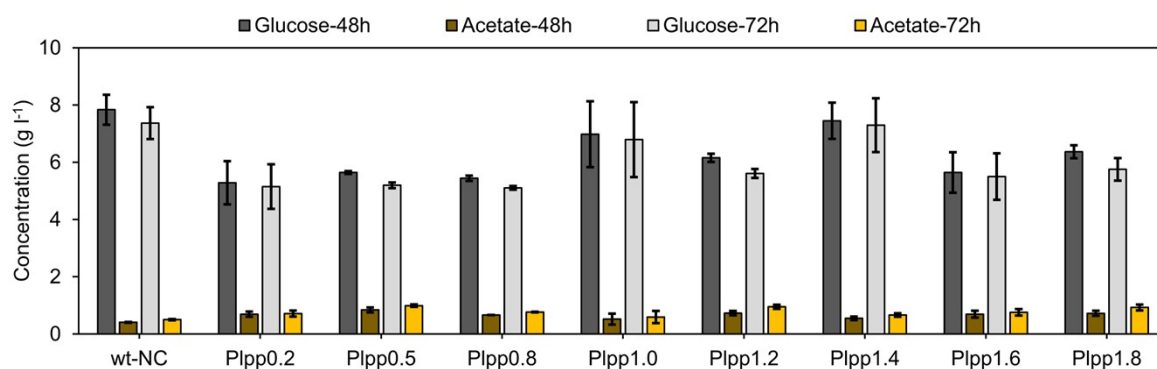


56

57 **Fig. S3. Comparison of 3HB production with or without P_{LlacO1} -controlled LIPK and**
 58 **BaPK based NOG pathway.** Shake flask experiments were performed with wildtype *E. coli*
 59 BW25113 (F') (wt) and its derived mutant strain J03 for 48 h and 72 h. Data indicated the
 60 mean \pm standard deviation ($n = 3$ independent biological replicates).

61

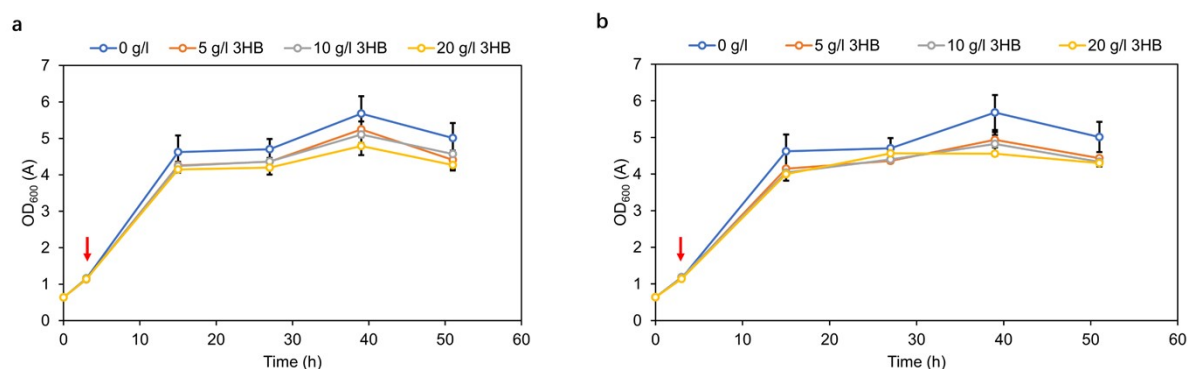
62



63

64 **Fig. S4. Glucose remaining and acetate accumulation during 3HB production via P_{Ippx} -**
 65 **tuned LIPK-based NOG pathway in strain J03.** Samples from 48 h and 72 h cultivation were
 66 analyzed by HPLC analysis. Data indicated the mean \pm standard deviation ($n = 3$ independent
 67 biological replicates).

68



69

70 **Fig. S5. Test of the 3HB and 1,3-BDO toxicity to *E. coli* BW25113 (F').** 3HB (a) or 1,3-
 71 BDO (b) with different concentrations (0-20 g l⁻¹) was fed to BW25113 (F') at 3 h post

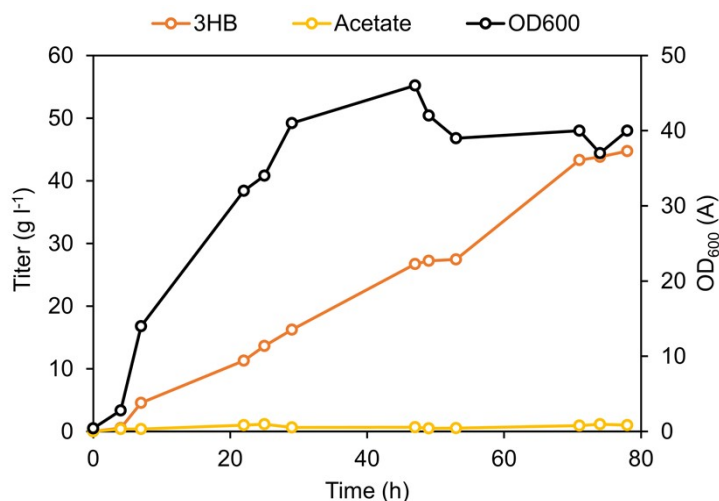
72 inoculation as indicated by the red arrows. Data indicated the mean \pm standard deviation ($n = 3$
73 independent biological replicates).

74

75

76

77



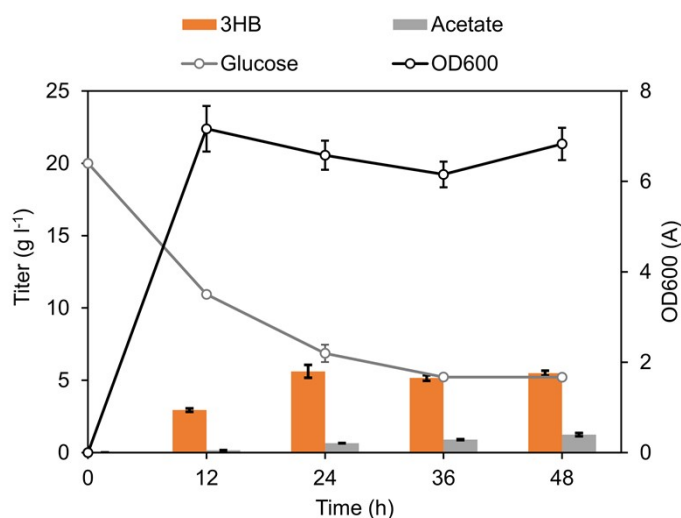
78

79 **Fig. S6. A duplicate run of fed-batch cultivation of J03 containing p3HB and pZLPK1.4**
80 **in 1-l bioreactor.**

81

82

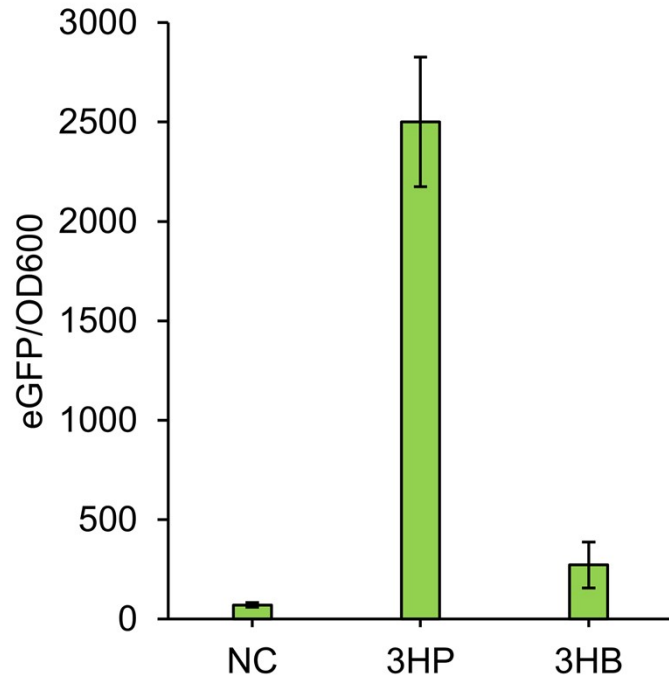
83



84

85 **Fig. S7. 3HB production via strain J06 harboring chromosomally integrated 3HB**
86 **pathway.** Data indicated the mean \pm standard deviation ($n = 3$ independent biological
87 replicates).

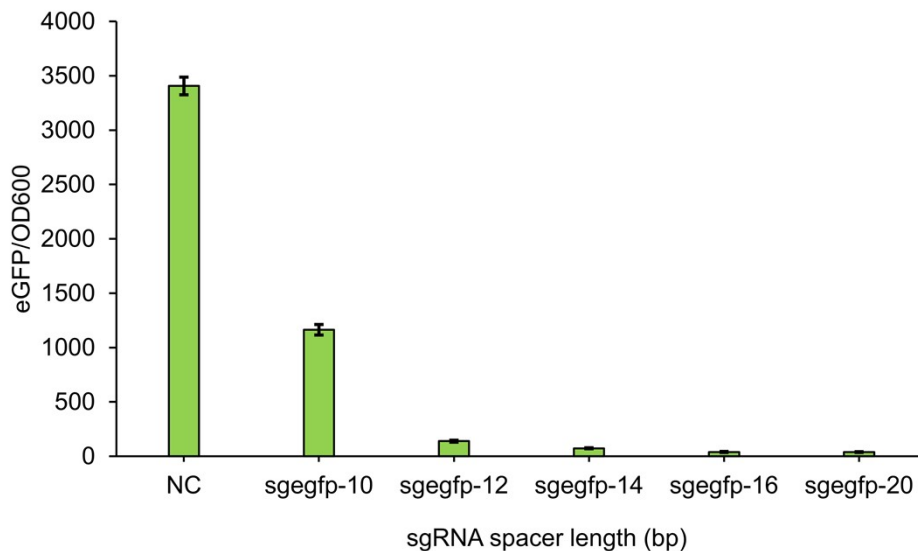
88



89

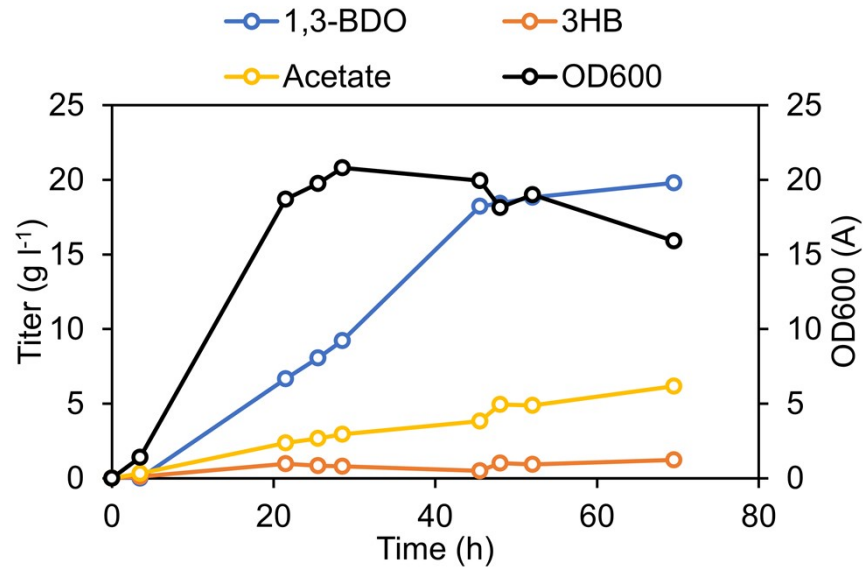
90 **Fig. S8. Induction of wildtype HpdR/P_{hpdH} sensor regulator system by 3HP and 3HB.** The
 91 eGFP induction assay was performed with strain *E. coli* BW25113 (F') harboring pZE-HpdR-
 92 PhpdH-eGFP. 3HP and 3HB were added at a final concentration of 1 g l⁻¹. NC indicates the
 93 negative control without any inducer. Data indicated the mean ± standard deviation (*n* = 3
 94 independent biological replicates).

95



96

97 **Fig. S9. Effects of spacer length on CRISPRi.** The eGFP repression assay was performed
 98 with strain J07 transformed with pZE-eGFP and pCS-sgRNA harboring sgegfp with spacer
 99 length of 10, 12, 14, 16, and 20 bp. NC indicates the negative control with pZE-eGFP and
 100 pCS27. Data indicated the mean ± standard deviation (*n* = 3 independent biological replicates).
 101



102

103 **Fig. S10. A duplicate run of fed-batch cultivation of J07 containing pZE-MaCAR, pCS-**
 104 **V1-*sgaccA-14* and pSLPK0.5 in 1-l bioreactor.**

105

106 **Table S1. Reactions and performance of various carbon metabolism involved in this**
 107 **study.**

Carbon Metabolism ^a	Metabolites per glucose	N/A stoichiometry ^b	C-yield ^c
EMP	2Acetyl-CoA+2CO ₂ +4NADH+2ATP	2	66.7%
PP	1.67Acetyl-CoA+2.67CO ₂ +3.33NADH+2NADPH+1.67ATP	3.19	55.7%
NOG	3Acetyl-CoA-1ATP	0	100%
EMP+PP	1.835Acetyl-CoA+2.335CO ₂ +3.665NADH+1NADPH+1.835ATP	2.54	61.2%
EMP+NOG	2.5Acetyl-CoA+1CO ₂ + 2NADH+0.5ATP	0.8	83.3%
PP+NOG	2.335Acetyl-CoA+1.335CO ₂ +1.67NADH+1NADPH+0.335ATP	1.14	77.8%
EMP+PP+NOG	2.223Acetyl-CoA+1.556CO ₂ +2.443NADH+0.67NADPH+0.89ATP	1.4	74.1%

108 ^a Glucose flux are presumed to equally enter the combined carbon metabolisms referred.

109 ^b NAD(P)H/acetyl-CoA stoichiometry.

110 ^c C-yield, or carbon yield, is the ratio of carbon in product acetyl-CoA to carbon in glucose.

111 **Table S2. Metabolic pathways for acetyl-CoA derived products involved in this study.**

Product pathways	Metabolic reactions	N/A stoichiometry
3HB	$2 \text{ Acetyl-CoA} + 1 \text{ NADH} \rightarrow 3\text{HB} + 1 \text{ NAD}^+$	0.5
1,3-BDO	$2 \text{ Acetyl-CoA} + 1 \text{ NADH} + 2 \text{ NADPH} + 1 \text{ ATP} \rightarrow 1,3\text{-BDO} + 1 \text{ NAD}^+ + 2 \text{ NADP}^+ + 1 \text{ AMP} + 1 \text{ PPi}$	1.5

112

113 **Table S3. Stoichiometric coefficients in equation (1) with multiple carbon metabolisms ^a.**

Product pathways	NADPH (a)	Product (b)	ATP (c)	NADH (d)	CO ₂ (e)
3HB	2y	-0.5x-0.67y+1.5	3x+2.67y-1	4.5x+4y-1.5	2x+2.67y
1,3-BDO	x+3.33y-3	-0.5x-0.67y+1.5	4x+4y-4 ^b	4.5x+4y-1.5	2x+2.67y

114 ^a 1 mol glucose is metabolized via three carbon metabolisms including EMP pathway (x mol),
 115 PP pathway (y mol) and NOG pathway ((1-x-y) mol). ^b Two ATP inputs were needed
 116 considering the additional need of an additional ATP for regeneration of AMP to ADP.
 117

118 **Table S4. Pathway yields for acetyl-CoA derived products with coordinated carbon**
 119 **metabolism.**

Products	NADPH (a)	NADPH (a)	Product (b)	ATP (c)	NADH (d)	CO ₂ (e)	Pathway yields (Y ^p) ^b
	1 EMP ^a	0.00	1.000	2.00	3.00	2.00	1.00
	1 PP	2.00	0.830	1.67	2.50	2.67	0.83
3HB	0.33 EMP+0.67 NOG	0.00	1.33	0.00	0.00	0.67	1.33
	0.38 PP+0.62 NOG	0.76	1.25	0.00	0.00	1.00	1.25
	1 EMP	-2.00	1.00	0.00	3.00	2.00	1.00
	1 PP	0.33	0.83	0.00	2.50	2.67	0.83
	0.75 PP+0.25 NOG	-0.50	1.00	-1.00	1.50	2.00	0.96
1,3-BDO	0.82 EMP+0.18NOG	-2.18	1.09	-0.72	2.19	1.64	1.05
	0.46 EMP+0.27PP+0.27 NOG	-1.64	1.09	-1.08	1.65	1.64	1.05

120 ^a Mol of glucose entering each carbon metabolism.

121 ^b The pathway yields (Y^p) were obtained from equation (4) in Supplementary Note
 122 considering NADH and NADPH are interconvertible.

123

124

125 **Table S5. Biochemical reactions for maximal glucose-to-product conversion with**
126 **coordinated carbon metabolism.**

Product pathways	Biochemical reactions
3HB	Glucose \rightarrow 1.33 3HB + 0.67 CO ₂
1,3-BDO	Glucose \rightarrow 1.05 1,3-BDO + 1.80 CO ₂

127

128 **Table S6. Specific activities of purified His₆-tagged phosphoketolases from different**
 129 **microorganisms.**

130 One unit of enzyme activity (U) is defined as conversion of 1 μmol of substrate per minute.

131 For R5P as the substrate, additional enzyme Rpe and RpiA was added at ten-fold

132 concentration of PK.

133

PK	Organisms	Substrates (10 mM)	Specific Activity (μmol/min/mg protein)
BaPK	<i>Bifidobacterium adolescentis</i>	F6P	8.42
		R5P	9.17
LlPK	<i>Lactococcus lactis</i>	F6P	7.26
		R5P	14.06
LcPK	<i>Lactobacillus casei</i>	F6P	6.54
		R5P	11.22
PaPK	<i>Pseudomonas aeruginosa</i> PAO1	F6P	5.54
		R5P	5.43
SyPK	<i>Synechocystis</i> sp. PC 6803	F6P	4.69
		R5P	5.73

134

135

136

137 **Table S7. Kinetic parameters of CARs towards 3-hydroxybutyrate.**

Enzyme	K_m (mM)	k_{cat} (min⁻¹)	k_{cat}/K_m (mM⁻¹min⁻¹)
MmCAR	17.22±3.13	10.86±0.88	0.61
MaCAR	10.87±3.30	19.00±2.86	1.75

138

139

140

141 **Table S8. Nucleotide sequence of HpdR/P_{hpdH} wildtype or variant promoters.**

Plasmids	Nucleotide Sequences
wt	(HpdR...) cat gcttgctctttatggcagttcggtc cggcctcttaacgggcatgccacaggtgcggtgaa cacctgaaggtaacgtgatccctgagctgcggcgagcccgtgaagaggtcgg tacaggctgcccctgt gctaaaacgcacagcggctgcgcgaaatctcgtgttccatccacgaaattactcactaagatggatc gggac aagaataaaaaacgaattcattaagaggagaaaggtacc ATG (...eGFP)
V1	(HpdR...) cat gcttgctctttatggcagttcggtc GTCGAC tacaggctgcccctgtgctaaaacgc acagcggctgcgcgaaatctcgtgttccatccacgaaattactcactaagatggatc gggacaagaataaaa aacgaattcattaagaggagaaaggtacc ATG (...eGFP)
V2	(HpdR...) cat ggtacctttcctctttaaatacaattccggttacaagtattacacaaagttttatgttgaga atattttttgat GTCGAC tacaggctgcccctgtgctaaaacgcacagcggctgcgcgaaatctcgtgt ttcatccacgaaattactcactaagatggatc gggacaagaataaaaaacgaattcattaagaggagaaag gtacc ATG (...eGFP)
V3	(HpdR...) cat gcttgctctttatggcagttcggtc GTCGAC tacaggctgcccctgtgctaaaacgc acagcggctgcgcgaaatctcgtgt tgacac cacgaaattactcac gatact ggatc gggacaagaataaaa aacgaattcattaagaggagaaaggtacc ATG (...eGFP)

142 Note: Bold triple nucleotides are start codons; nucleotides in red lower cases are the putative
143 palindromic sequence (-209 to -118 bp); nucleotides in red upper cases denote *SaI* restriction
144 site; nucleotides in grey shade denote -35 and -10 boxes in wildtype P_{hpdH} promoter;
145 nucleotides in green shade denote substituted -35 and -10 boxes from P_{LlacO1} promoter;
146 nucleotide in yellow shade is the transcription initiation site on P_{hpdH} promoter.

147 **Table S9. Strains and plasmids used in this study.**

Strains	Properties	Source
<i>E. coli</i> XL1-Blue	<i>recA1 endA1 gyrA96 thi-1 hsdR17 supE44 relA1 lac F'</i> [<i>traD36 proAB lacI^qZΔM15 Tn10 (Tet^r)</i>]	Stratagene
<i>E. coli</i> BL21 Star(DE3)	F ⁻ <i>ompT hsdSB (rB-mB-) gal dcm rne131</i> (DE3)	Invitrogen
<i>E. coli</i> BW25113 (F')	<i>rrnBT14 ΔlacZWJ16 hsdR514 ΔaraBADAH33 ΔrhaBADLD78 F'</i> [<i>traD36 proAB lacI^qZΔM15 Tn10(Tet^r)</i>]	2
J01	<i>E. coli</i> BW25113 (F') Δ <i>edd</i>	This study
J02	<i>E. coli</i> BW25113 (F') Δ <i>edd</i> Δ <i>pfkA</i>	This study
J03	<i>E. coli</i> BW25113 (F') Δ <i>edd</i> Δ <i>pfkB</i>	This study
J04	<i>E. coli</i> BW25113 (F') Δ <i>edd</i> Δ <i>pfkA</i> Δ <i>zwf</i>	This study
J05	<i>E. coli</i> BW25113 (F') Δ <i>edd</i> Δ <i>pfkB</i> Δ <i>zwf</i>	This study
J06	J03 with the 3HB pathway integrated into the genome at <i>asl</i> locus	This study
J07	J06 with <i>P_LlacO1</i> -dCas9 integrated into the genome at <i>dkgB</i> locus	This study
Plasmids	Properties	Source
pETDuet-1	<i>PT7, pBR322 ori, Amp^r</i>	Novagen
pZE12-luc	<i>P_LlacO1, colE ori, Amp^r</i>	3
pCS27	<i>P_LlacO1, P15A ori, Kan^r</i>	4
pSA74	<i>P_LlacO1, pSC101* ori, Cl^r</i>	5
pSA-dCas9	pSA74 harboring dCas9 from <i>Streptococcus pyogenes</i>	6
pCS-sgRNA	pCS27 harboring sgRNA targeting eGFP	6
pZE-eGFP	pZE12-luc harboring eGFP	This study
pZE-MmCAR	pZE12-luc harboring <i>car</i> from <i>Mycobacterium marinum</i> M and <i>sfp</i> amplified from <i>Bacillus subtilis</i> 168	7
pZE-MaCAR	pZE12-luc harboring <i>car</i> from <i>Mycobacterium abscessus</i> and <i>sfp</i> amplified from <i>Bacillus subtilis</i> 168	This study
pZE-LIPK- <i>glpX</i>	pZE12-luc harboring phosphoketolase (LIPK, KST82569.1) from <i>Lactococcus lactis</i> NCTC 6681, <i>glpX</i> from <i>E. coli</i>	This study

pZE-BaPK- <i>glpX</i>	pZE12-luc harboring phosphoketolase (BaPK, BAF39468.1) from <i>Bifidobacterium adolescentis</i> ATCC 15703, <i>glpX</i> from <i>E. coli</i>	This study
pZLPK	pZE12-luc harboring phosphoketolase (LIPK, KST82569.1) from <i>Lactococcus lactis</i> NCTC 6681, <i>glpX</i> and <i>tktA</i> from <i>E. coli</i>	This study
pZBPK	pZE12-luc harboring phosphoketolase (BaPK, BAF39468.1) from <i>Bifidobacterium adolescentis</i> ATCC 15703, <i>glpX</i> and <i>tktA</i> from <i>E. coli</i>	This study
pZLPKx	pZE12-luc harboring LIPK, <i>glpX</i> and <i>tktA</i> from <i>E. coli</i> under control of constitutive promoter library Plppx	This study
pSLPKx	pSA74 harboring LIPK, <i>glpX</i> and <i>tktA</i> from <i>E. coli</i> under control of constitutive promoter library Plppx	This study
p3HB	pCS27 carrying <i>thl</i> and <i>hbd</i> from <i>Clostridium difficile</i> 630 and <i>tesB</i> from <i>E. coli</i>	This study
pETDuet-MmCAR	pETDuet-1 harboring <i>car</i> from <i>Mycobacterium marinum</i> M and <i>sfp</i> amplified from <i>Bacillus subtilis</i> 168	This study
pETDuet-MaCAR	pETDuet-1 harboring <i>car</i> from <i>Mycobacterium abscessus</i> and <i>sfp</i> amplified from <i>Bacillus subtilis</i> 168	This study
pETDuet-BaPK	pETDuet-1 harboring BaPK from <i>Bifidobacterium adolescentis</i>	This study
pETDuet-LIPK	pETDuet-1 harboring LIPK from <i>Lactococcus lactis</i>	This study
pETDuet-LcPK	pETDuet-1 harboring LcPK from <i>Lactobacillus casei</i>	This study
pETDuet-PaPK	pETDuet-1 harboring PaPK from <i>Pseudomonas aeruginosa</i>	This study
pETDuet-SyPK	pETDuet-1 harboring SyPK from <i>Synechocystis sp.</i> PCC 6803	This study
pETDuet-Rpi	pETDuet-1 harboring <i>rpi</i> from <i>E. coli</i>	This study
pETDuet-Rpe	pETDuet-1 harboring <i>rpe</i> from <i>E. coli</i>	This study
pZE-HpdR-eGFP	pZE12-luc containing HpdR- P_{hpdH} from <i>Pseudomonas putida</i> and eGFP	This study
pCS-wt	pCS27 containing HpdR- P_{hpdH} -eGFP	This study
pCS-V1	pCS-wt with deletion of a palindromic sequence (-209 to -118 bp) on the P_{hpdH} promoter	This study
pCS-V2	pCS-V1 with HpdR under control of $P_{lpp1.0}$ promoter	This study
pCS-V3	pCS-V1 by substituting the -35 and -10 boxes of P_{hpdH} promoter with those from P_{lacO1} promoter	This study
pCS- <i>sgegfp-20</i>	pCS-sgRNA containing <i>sgegfp</i> with 20 bp spacer targeting eGFP at the start codon region with a TGG PAM site	This study
pCS- <i>sgegfp-16</i>	pCS-sgRNA containing <i>sgegfp</i> with 16 bp spacer targeting eGFP at the start codon region with a TGG PAM site	This study
pCS- <i>sgegfp-14</i>	pCS-sgRNA containing <i>sgegfp</i> with 14 bp spacer targeting eGFP at the start codon region with a TGG	This study

	PAM site	
pCS- <i>sgegfp-12</i>	pCS-sgRNA containing <i>sgegfp</i> with 12 bp spacer targeting eGFP at the start codon region with a TGG PAM site	This study
pCS- <i>sgegfp-10</i>	pCS-sgRNA containing <i>sgegfp</i> with 10 bp spacer targeting eGFP at the start codon region with a TGG PAM site	This study
pCS-V1- <i>sgaccA-14</i>	pCS-V1 harboring sgRNA targeting <i>accA</i> with 14 bp spacer	This study
pCS-V1- <i>sgaccA-12</i>	pCS-V1 harboring sgRNA targeting <i>accA</i> with 12 bp spacer	This study
pCS-V1- <i>sgaccA-10</i>	pCS-V1 harboring sgRNA targeting <i>accA</i> with 10 bp spacer	This study
pCS-V2- <i>sgfabD-14</i>	pCS-V2 harboring sgRNA targeting <i>fabD</i> with 14 bp spacer	This study
pCS-V2- <i>sgaccA-12</i>	pCS-V2 harboring sgRNA targeting <i>fabD</i> with 12 bp spacer	This study
pCS-V2- <i>sgaccA-10</i>	pCS-V2 harboring sgRNA targeting <i>fabD</i> with 10 bp spacer	This study

148

149

150 **Reference**

- 151 1. D. Dugar and G. Stephanopoulos, *Nat. Biotechnol.*, 2011, **29**, 1074-1078.
152 2. S. Atsumi, A. F. Cann, M. R. Connor, C. R. Shen, K. M. Smith, M. P. Brynildsen, K.
153 J. Chou, T. Hanai and J. C. Liao, *Metab. Eng.*, 2008, **10**, 305-311.
154 3. R. Lutz and H. Bujard, *Nucleic Acids Res.*, 1997, **25**, 1203-1210.
155 4. C. R. Shen and J. C. Liao, *Metab. Eng.*, 2008, **10**, 312-320.
156 5. Y.-X. Huo, K. M. Cho, J. G. L. Rivera, E. Monte, C. R. Shen, Y. Yan and J. C. Liao,
157 *Nat. Biotechnol.*, 2011, **29**, 346-351.
158 6. J. Wang, Y. Wu, X. Sun, Q. Yuan and Y. Yan, *ACS Syn. Biol.*, 2017, **6**, 1922-1930.
159 7. Z. Chen, X. Sun, Y. Li, Y. Yan and Q. Yuan, *Metab. Eng.*, 2017, **39**, 102-109.

160